

Concerted Wire Lifting: Enabling Secure and Cost-Effective Split Manufacturing

Satwik Patnaik

Johann Knechtel

Mohammed Ashraf

Ozgur Sinanoglu

Tandon School of Engineering
New York University, USA
sp4012@nyu.edu

Design for Excellence Lab, Division of Engineering
New York University Abu Dhabi, UAE
{johann, ma199, ozgursin}@nyu.edu

Abstract—Here we advance the protection of split manufacturing (SM)-based layouts through the judicious and well-controlled handling of interconnects. Initially, we explore the cost-security trade-offs of SM, which are limiting its adoption. Aiming to resolve this issue, we propose effective and efficient strategies to lift nets to the BEOL. Towards this end, we design custom “elevating cells” which we also provide to the community. Further, we define and promote a new metric, Percentage of Netlist Recovery (PNR), which can quantify the resilience against gate-level theft of intellectual property (IP) in a manner more meaningful than established metrics. Our extensive experiments show that we outperform the recent protection schemes regarding security. For example, we reduce the correct connection rate to 0% for commonly considered benchmarks, which is a first in the literature. Besides, we induce reasonably low and controllable overheads on power, performance, and area (PPA). At the same time, we also help to lower the commercial cost incurred by SM.

I. INTRODUCTION

Nowadays, chip manufacturing is a complex and costly process, where more often than not third-party facilities are involved. As a result, protecting intellectual property (IP) as well as ensuring trust in the chips becomes challenging.

The IARPA agency proposed *split manufacturing (SM)* as a protection technique to ward off threats like IP piracy, unauthorized overproduction, and insertion of hardware Trojans [1]. In the simplest embodiment of SM, the FEOL is handled by a high-end, competitive off-shore fab which is potentially *untrusted*, while the BEOL is manufactured subsequently at a low-end, *trusted* facility (Fig. 1). Hill *et al.* [2] successfully demonstrated the viability of SM by fabricating a 1.3 million-transistor asynchronous FPGA. Further studies also bear testament to the applicability of SM [3, 4, 5]. However, the overall acceptance of SM remains behind expectations so far, mainly due to concerns about cost.

The protection offered by SM is based on the fact that the FEOL fab does not have access to the complete design, and an attacker *may* thus be hindered from malicious activities. The threat models for SM [6] are accordingly focused on FEOL-based adversaries which either seek to (i) retrieve the design and/or its IP, or (ii) insert hardware Trojans. Some studies also consider both at the same time [7, 8]. Here, we address (i).

Prior art suggests splitting after M1, as such a scenario forces an attacker to tackle a “vast sea of gates” with only a few transistor-level interconnects provided along [3]. Although splitting after M1 arguably provides the best protection, it also



Fig. 1. Concept of split manufacturing, i.e., the separation of a layout into the FEOL and BEOL parts. Note the different pitches across the metal layers. As the FEOL part is outsourced, it may require additional protection (such as placement perturbation or lifting of wires) against fab-based adversaries.

necessitates a high-end BEOL fab for trusted fabrication of all remaining metal layers, including the lower layers with very small pitches. Since this requirement may be considered too costly, some studies propose to split after M4 [7, 9, 10].¹ However, doing so can undermine security by revealing more structural connectivity information to an attacker [11, 12, 13].

The key challenge for SM is thus: *how to render split manufacturing practical regarding both security and cost?*

Here, we address this challenge with a secure and effective approach for SM. Our key principle is to lift wires to the BEOL in a controlled and concerted manner, considering both cost and security. Our work can be summarized as follows:

- Initially, we revisit the cost-security trade-offs for SM. We explore the prospects of wire lifting and find that naive lifting to higher metal layers can improve the security albeit at high layout cost. Thus, we proclaim the need for cost- and security-aware, concerted lifting schemes.
- We put forward multiple strategies to select and lift nets. The key ideas to achieve strong protection are (i) to increase the number of protected/lifted nets and (ii) to dissolve hints of physical proximity for those nets.
- Based on our strategies, we propose a method for the *concerted lifting of wires* with controllable impact on power, performance, and area (PPA). Since we lift wires to higher metal layers (M6, without loss of generality), our method also helps to lower the commercial cost of SM.

¹We advocate the terminology “to split after” instead of the commonly used “to split at.” For example, “to split at M2” remains ambiguous whether M2 is still within the FEOL or already in the BEOL. Further, the same uncertainty applies to the vias of V12 and V23, i.e., those between M1/M2 and M2/M3, respectively. Our definition for “to split after M2” is that M2 and V12 are still in the FEOL, while the vias of V23 are already in the BEOL.

- For the actual layout-level lifting, we design custom “elevating cells.” Unlike the prior art, our techniques allow to lift and route wires in a controlled manner in the BEOL.
- We promote a new metric, *Percentage of Netlist Recovery (PNR)*, which quantifies the resilience offered by any SM protection scheme against varying effective attacks.
- We conduct a thorough evaluation of layout cost and security on finalized layouts for various benchmarks, including the large-scale *IBM superblue* suite. We contrast the superior resilience of our layouts with prior protection schemes, and make our layouts publicly available, along with the library definition for elevating cells [14].

II. BACKGROUND AND MOTIVATION FOR OUR WORK

A. On Prior Studies and Some Limitations

Attack Schemes: Naive SM (i.e., splitting a layout as is) likely fails to avert skillful attackers. That is because physical design tools arrange gates to be connected as close as possible, subject to available routing resources and other constraints. Rajendran *et al.* [11] introduced the concept of *proximity attack* where that insight is exploited to infer undisclosed interconnects. More recently, Wang *et al.* [12] proposed a network-flow-based attack which utilizes further hints such as the direction of dangling wires and constraints on both load capacitances and delays. Magaña *et al.* [9, 10] utilized routing-based proximity in conjunction with placement-centric proximity.

Protection Schemes: Various techniques have been put forward to protect SM-based designs from proximity attacks. Swapping of block pins was proposed by Rajendran *et al.* [11] to obtain an unbiased *Hamming distance* of 50% between the outputs of the original netlist and the outputs of the netlist restored by an attacker. Wang *et al.* [12] proposed gate-level placement perturbation within an optimization framework, to maximize resilience and minimize wirelength overhead at the same time. Sengupta *et al.* [13] also pursued various placement perturbation techniques, along with a discussion on information leakage for SM. Wang *et al.* [15] proposed a routing-based protection scheme applying wire lifting, deliberate re-routing, and VLSI test principles, all to tailor the Hamming distance towards 50%. Magaña *et al.* [9, 10] advocated inserting routing blockages to lift wires and, thus, to mitigate routing-centric attacks as those proposed in their study.

Besides those studies addressing proximity attacks, Imeson *et al.* [16], Li *et al.* [17], and Chen *et al.* [18] focus on hardware Trojans. Patnaik *et al.* [19] pursue BEOL-centric and large-scale layout camouflaging; the authors note that their scheme is also promising in the context of split manufacturing.

Limitations of Protection Schemes: The approach of Rajendran *et al.* [11] is only applicable to hierarchical designs. More importantly, pin swapping is rather limited in practice; on average, 87% correct connections were reported in [11].

Placement-centric schemes would ideally (re-)arrange gates randomly, thereby “dissolving” any hint of spatial proximity. As this likely induces excessive PPA overheads [13, 16], placement perturbation is typically applied more carefully [12, 13]. However, as we reveal in Sec. VI, overly restricted perturbation can provide only a little protection, especially for splitting after higher layers.

TABLE I
PITCH DIMENSIONS FOR THE METAL LAYERS IN THE 45nm NODE [11].

Layer	M1	M2	M3	M4	M5	M6	M7	M8	M9	M10
Pitch (nm)	130	140	140	280	280	280	800	800	1600	1600

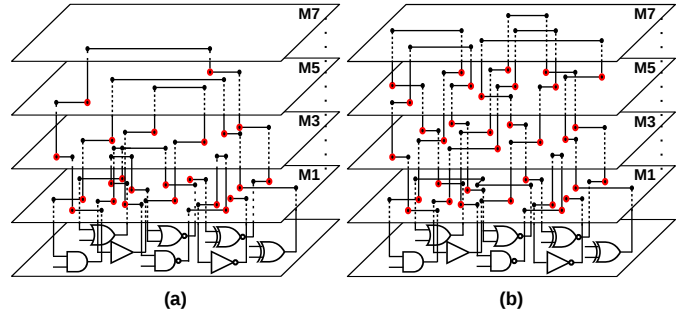


Fig. 2. (a) Conceptual illustration of a regular, unprotected layout. The red dots represent open pins, which would induce dangling wires once the layout is split at each respective layer. Note that the majority of nets are completed in lower layers, hence fewer open pins are observed for higher layers. (b) Conceptual illustration of a layout protected by wire lifting. Here the majority of nets are completed in M7 (without loss of generality). Hence, any split below M7 induces many open pins to be tackled by an attacker.

Similar to placement-centric schemes seeking to limit PPA overheads, some routing-based schemes such as [15] also protect only a small subset of the design (a few nets). These techniques are further subject to available routing resources, and re-routing may be restricted to short local detours which can be easy to resolve for an advanced attacker. Besides, implicit re-routing by insertion of blockages [9, 10] falls short of explicitly protecting selected nets and controlling the routing of wires.

B. On the Trade-Offs for Cost Versus Security

It is challenging to determine the most appropriate split layer as such a decision has direct and typically opposing impact on security and cost. Recall that some prior art promoted to split after lower metal layers. However, this comes at a high commercial cost for the trusted BEOL fab. In contrast, splitting after higher layers allows for large-pitch and low-end processing setups at the BEOL fab, thus reducing cost (but possibly undermining security). For example, considering the pitches for the 45nm node (Table I), one may prefer to split after M3 (or M6, or even M8) over splitting after M1.² Further aspects promoting higher split layers are also discussed in [7].

When a net is cut across FEOL and BEOL by SM, at least two *dangling wires* arise in the topmost layer of the FEOL.³ Dangling wires remain unconnected at one end; these open ends indicate the locations where the vias linking the FEOL and BEOL are to be manufactured (by the BEOL fab). We refer to those via locations as open pins (Fig. 2). Further, we define *open pin pairs (OPPs)* as pairs (p_d, p_s) where p_d is connected

²Splitting after other layers is also possible, but considering cost and applicability we suggest that any split should occur just below the next larger pitch. This way, the BEOL fab has to manufacture only those larger pitches.

³The reverse is not necessarily true, i.e., not all dangling wires represent a cut net—dangling wires may also be used for obfuscation. Such wires are routed in the FEOL but remain open in the BEOL; see also Sec. III. Besides, the number of dangling wires depends both on the net’s pin count and how/where exactly it is cut. See also Fig. 6 for an illustrative example.

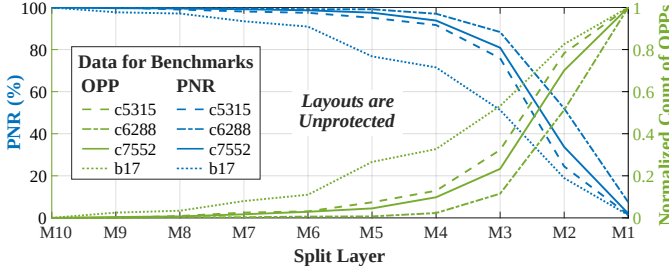


Fig. 3. Percentage of netlist recovery (PNR, see also Sec. V) versus open pin pairs (OPPs), plotted as a function of the split layer. Note that the split layers are ordered from M10 to M1. The unprotected layouts are naively split as is and the attack is based on [12].

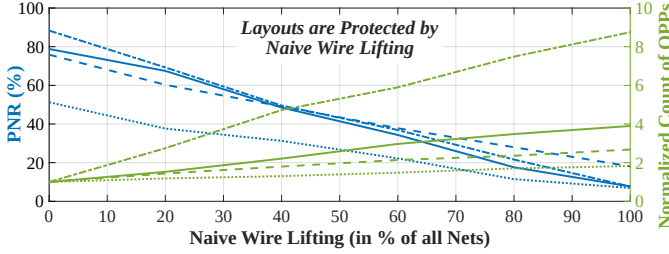


Fig. 4. PNR versus OPPs, plotted as a function of randomly selected nets lifted to M6. The set of benchmarks and the legend are the same as in Fig. 3. The protected layouts are split after M3 and the attack is based on [12]. The OPP baselines (normalized OPP count of 1.0) are derived from each respectively unprotected layout, i.e., where 0% of all nets are lifted.

to a driver and p_s to at least one sink. The related routing is observable in the FEOL, but the true mapping of drivers to sinks is comprehensible only with the help of the BEOL.

For an attacker operating at the FEOL, observing fewer OPPs directly translates to a reduced solution space and, thus, may lower her/his efforts for recovery of the protected design. In Fig. 3, we plot an attacker’s success rate versus the OPP count for various split layers. There are strongly reciprocal correlations across the layers, confirming that layouts split after higher layers are much easier to attack. That is because more and more nets are routed completely within the FEOL once we split after higher layers. Naturally, these FEOL-routed nets yield no OPPs and, hence, impose no efforts for the attack.

One way to enforce many OPPs while splitting only after higher layers is *wire lifting*, i.e., the deliberate routing of nets towards and within the BEOL (Figs. 2 and 4). There is a common concern of overly large PPA cost for large-scale wire lifting [8, 16]. We confirm this in Fig. 5, where we plot PPA over-

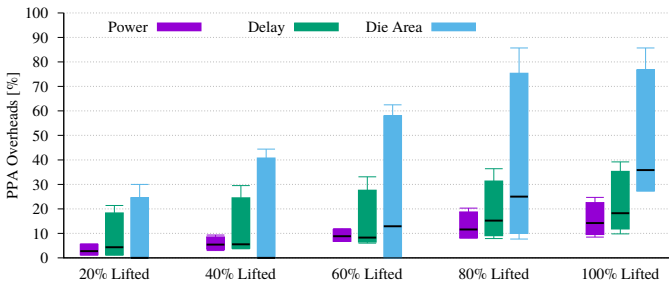


Fig. 5. PPA overheads for naive lifting of randomly selected nets to M6. The plot is based on the same benchmarks as in Fig. 3. The boxes span from the 5th to the 95th percentile, the whiskers represent the minimal and maximal values, and the black bars represent the medians, respectively.

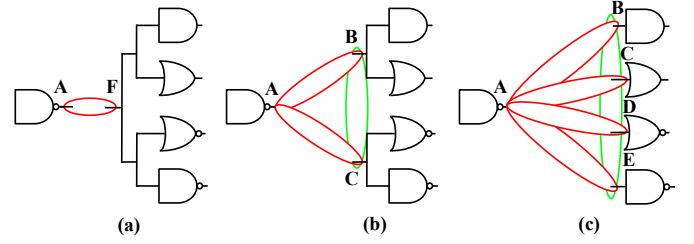


Fig. 6. The impact of lifting high-fanout nets on the number of open pin pairs.

heads for *naive lifting* of randomly selected nets.⁴ Note that the die area is particularly impacted. That is because lifting more and more wires in an uncontrolled manner induces notable routing congestion which, in order to obtain DRC-clean layouts, can only be managed by enlarging the die outlines.

Overall, there is a need for an *SM scheme ensuring a large number of OPPs, while splitting after higher layers (at low commercial cost), but without inducing excessive PPA cost*. We believe that such a scheme will expedite the acceptance of SM in the industry. In this work, we propose such a scheme through the notion of *concerted wire lifting*.

III. STRATEGIES FOR CONCERTED WIRE LIFTING

As motivated in Sec. II-B, the number of OPPs in the FEOL should be as large as possible, but not at high cost—pertaining to commercial and PPA cost. We tackle this problem with the help of our custom *elevating cells* (ECs). The key idea of routing nets through ECs is to establish pins in the metal layer of choice (above the split layer), thereby inducing OPPs for those nets. (See Sec. IV and Fig. 10 for implementation details.)

Next, we introduce our strategies for concerted wire lifting. They are based on exploratory but comprehensive layout-level experiments. These strategies outperform naive lifting as well as recent prior art regarding security while inducing only little PPA overhead at the same time (see Sec. VI).

Strategy 1, Lifting High-Fanout Nets: We begin by lifting high-fanout nets (HiFONs) for two reasons: (i) any wrong connection made by an attacker propagates the error to multiple locations, and (ii) lifting HiFONs helps introduce many OPPs. We define nets with two or more sinks as HiFONs.⁵

Consider Fig. 6 as an example. Here, a HiFON is originally connecting to four gates/sinks. Depending on how and where the HiFON is lifted, the attacker has different scenarios to cope with. In (a), only one OPP arises which is trivial to attack/resolve. In (b), two OPPs are to be tackled, (A,B) and (A,C). Assuming that an attacker cannot tell how many sinks *exactly* to consider,⁶ either one of the two OPPs or both OPPs at the same time are equally likely representing the original net.

⁴We implement naive lifting by placing one “elevating cell” next to the driver; see Secs. III and IV for details on those cells and their use. Such naive lifting enforces routing at least to some degree above the split layer, thereby inducing OPPs and hampering an attacker’s recovery rate (Fig. 4). However, naive lifting cannot handle OPPs in a controlled manner.

⁵Although large fanouts may be subject to timing-driven optimization such as buffering or cloning [20], we found that on average 20–30% of all the nets in the benchmarks we consider have a fanout of at least 2. In any case, our techniques are generic and can be readily applied for any degree of fanout.

⁶While a skillful attacker may understand the driving strengths of any gate, she/he cannot easily resolve their original use given only the FEOL. Any high-strength driver may have to be reconnected either to many sinks nearby or

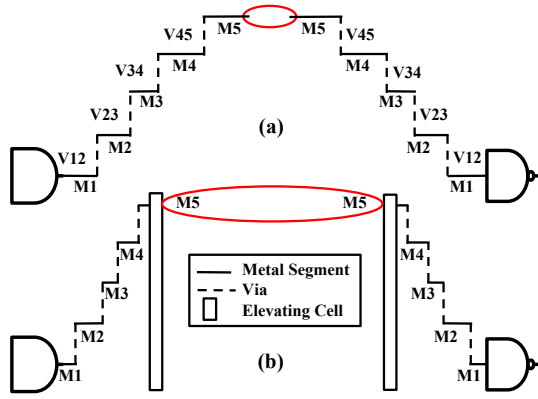


Fig. 7. Distances for open pin pairs (OPPs). In (a), only a short distance arises due to implicit wire lifting, whereas in (b) we precisely control the distance using two elevating cells (ECs).

Thus, the attacker has three options to consider. In (c), even up to 14 options arise; there are four OPPs (A,B), (A,C), (A,D), and (A,E), as well as 10 possible combinations of those OPPs. Naturally, once other nets are lifted as well, the set of OPPs scales up even further, in fact in a combinatorial manner.

We lift all wires of any HiFON (Fig. 6(c)), to induce as many OPPs as possible. We do so by inserting separate ECs for the driver as well as for all the sinks.

Strategy 2, Controlling the Distances for OPPs: Besides increasing the number of OPPs, it is also necessary to control the distances between their pins. For example in Fig. 7(a), only a short open remains in M5 for the lifted wire/net, motivating an attacker to reconnect that particular OPP. Such a scenario may arise for implicit wire lifting, e.g., as proposed in [9, 10]. There, only the FEOL metal layers to avoid are declared, but the actual routing paths in the BEOL layers are not.

In our method, we can control the distances for OPPs at will, simply by controlling the placement of the ECs (Figs. 7(b)). We place ECs close to the driver and the sink(s), thereby enlarging the distances and increasing an attacker’s efforts. To mitigate any advanced attack, e.g., based on learning the distance distribution for OPPs while reverse-engineering other available chips, one may also place the ECs randomly within (or even beyond) the bounding boxes of the nets.

Strategy 3, Obfuscation of Short Nets: Above we assumed that enlarging the distances of OPPs is practical and effective, which is straightforward for HiFONs (as well as for relatively long nets). For short nets, however, enlarging those distances requires some routing detours out of the net’s bounding box. Furthermore, short nets may be easy for an attacker to identify and localize, based on the typically low driver strength. To tackle both issues, we design another EC (Figs. 8 and 10(b)).

This EC places two pins close to each other: one “true” pin is connected to the short net’s driver, and the other “dummy” pin is connected to a randomly but carefully selected gate, representing a dummy driver. An attacker cannot easily distinguish these two drivers: (i) the dummy driver is selected such that no combinatorial loops would arise were the driver connected to the short net’s sink(s), and (ii) we adapt both drivers’ strength, also accounting for the routing detours, via ECO optimizations.

to few sinks far away. Given that wire lifting is conducted across the whole layout, drivers and sinks of various nets will be “spatially intermixed,” notably increasing an attacker’s efforts to map drivers to sinks correctly.

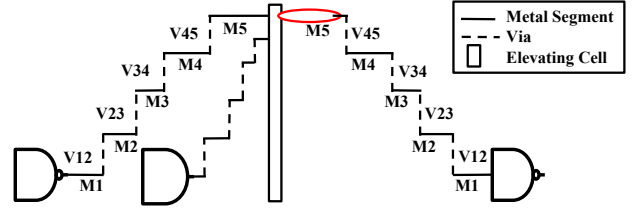


Fig. 8. We obfuscate short nets by connecting the real and dummy driver to another, dedicated type of EC. The dummy driver’s wire connected with the EC is left dangling beyond the split layer. Note that the dummy driver is a real driver for another net; the related wires are not illustrated here. Both drivers’ strengths are adapted such that they might seemingly connect to the sink of the obfuscated short net. The EC is placed between the real and the dummy driver, thereby increasing the OPP distances.

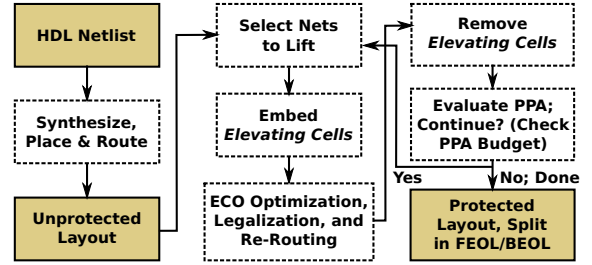


Fig. 9. The flow of our protection scheme.

Besides obfuscation, this EC induces a *dummy OPP* which naturally increases the overall number of OPPs.

Note that we insert only one EC for short nets, specifically between their real and dummy driver. We refrain from inserting another EC near the sink of short nets, as we observed that doing so contributes little for security but hampers routability.

IV. METHODOLOGY

Next, we discuss our methodology (Fig. 9), which is integrated with *Cadence Innovus* using custom in-house scripts. Given an HDL netlist, we first synthesize, place, and route the design. The resulting layout is protected as follows. For each net we wish to lift, *elevating cells* (EC) are temporarily inserted next to the net’s driver (as well as next to all the net’s sinks for HiFONs and long nets). It is important to note that ECs do not impact the FEOL device layer; they are designed to solely elevate/lift a given net. Next, we perform ECO optimization and legalization based on customized scripts. Then, we re-route the design, remove the ECs, extract the RC information, and report the PPA numbers. In case the PPA budget allows for additional wire lifting, we continue iteratively. Finally, a DEF file split into FEOL/BEOL is exported for security analysis against proximity attacks.

Strategy for Selecting Nets to Lift: In general, we lift nets according to the strategies discussed in Sec. III. More specifically, considering the iterative flow outlined above, we take the following steps to determine all nets to be lifted.

1. Given a ratio of nets to lift, we initially lift HiFONs and then long nets using Strategies 1 and 2. Here we prioritize HiFONs based on their fanout degree; large-fanout HiFONs are lifted first. Furthermore, it is easy to see that the longer a net, the more freedom we have for controlling its OPP distance(s), and the less likely it is for an attacker

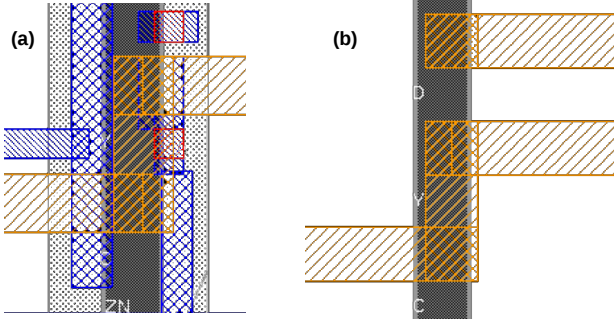


Fig. 10. Post-processed snapshots of our two types of ECs. Wires in M6 are in orange, wires/vias in M1 are in blue/red. In (a), the EC (dark grey) is seen overlapping an inverter (light grey, dotted). In (b), the EC is seen alone; this EC has two inputs (C, D), as required for obfuscation of short nets. Recall that the OPPs arise after the split layer, i.e., below M6—OPP are not visible here.

to reconnect that net successfully. Therefore, we prioritize nets not already lifted as HiFONs by their wirelength.

2. We then lift short nets using Strategy 3, until a given PPA budget is utilized. We prioritize nets based on their wirelength—the shortest nets are selected first. That is because the shorter a net, the easier it is to successfully reconnect by an attacker. Since the additional wires required to connect with dummy drivers consume notable routing resources, we lift short nets in small steps of 10% and iteratively monitor the PPA impact.

Design of Elevating Cells: As with any custom cell, our ECs are embedded in a library of choice. We make our EC implementation for the *Nangate 45nm* library publicly available in [14]. Fig. 10 illustrates the two different types of ECs. The key properties of our ECs are discussed next.

1. All I/O pins are set up in one metal layer. Since the pins must reside above the split layer to effectuate wire lifting, we implement different ECs as needed for various layers.
2. The pin dimensions and offsets are chosen such that the pins can be placed onto the respective metal layer's tracks. This helps minimize the routing congestion.
3. ECs may overlap with any other standard cell (Fig 10(a)). That is because the latter have their pins exclusively in lower metal layers, whereas ECs neither impact those layers nor the FEOL device layer.
4. Custom legalization scripts have been set up to prevent the pins of different ECs to overlap with each other.
5. Timing and power characteristics of a *BUF2X* cell (buffer with driving strength 2) are leveraged for the ECs. A detailed library characterization is not required since ECs only translate to some interconnects in the BEOL.
6. To enable proper ECO optimization, the ECs are set up for load annotation at design time. That is required to capture the capacitive load of (i) the wire running from the EC to the sink and (ii) the sink itself. Note that this annotation is also essential for obfuscating the dummy drivers' strength as outlined in Strategy 3 (Sec. III).

V. METRICS FOR LAYOUT PROTECTION

Here we discuss metrics to gauge the resilience of layouts when accounting for FEOL-based attacks. First we review established metrics and then we introduce a novel metric.

The **Hamming Distance (HD)** quantifies the average bit-level mismatch between the outputs of the original and the attacker's reconstructed design [11]. Note that the HD reveals the degree of functional mismatch, but not necessarily structural mismatches. (That is because any Boolean function can be represented by different gate-level designs.) Hence, the HD cannot adequately quantify the potential for gate-level IP theft.

The **Output Error Rate (OER)** indicates the probability for any bit per output being wrong while applying a possibly large set of inputs to the attacker's netlist [12, 15]. As this metric tends to approach 100% for any imperfect attack, it does not reflect well on the degree and type of errors made by an attacker, but rather whether any error was made at all. Like the HD, it should not be used to quantify the gate-level resilience.

The **Correct Connection Rate (CCR)** is the ratio of connections correctly inferred by an attacker over the number of protected nets. For example, if 20 out of 100 protected nets are correctly reconnected, the CCR is 20%. Note that Wang *et al.* [15] defined an *Incorrect Connection Rate (ICR)*, which is simply the inverse of this metric. Unlike the HD or OER, this metric can quantify the gate-level protection (or its failure).

Our metric **Percentage of Netlist Recovery (PNR)** captures the ratio of correctly inferred connections over the total number of nets. It quantifies the structural similarity between the original netlist and the attacker's netlist. Thus, the PNR is more generic and comprehensive than the CCR, as it accounts for the entire netlist, not only for protected nets. Vice versa, the CCR can be considered a special case of the PNR. For unprotected layouts, both metrics shall be equal by definition.

For example, consider again that an attacker reconstructs 20 out of 100 protected nets, out of 10,000 nets in total. Now consider further that an attacker can readily identify all nets completely routed in the FEOL. Assuming that 2,000 nets are routed in the FEOL, the PNR would be 20.2%. For 6,000 nets routed in the FEOL, however, the PNR would be already 60.2%—while the CCR remains 20% for both cases.

In short, the PNR quantifies (i) the overall potential of IP theft and (ii) the resilience of any SM protection scheme against varying effective attacks, and for varying split layers.

VI. EXPERIMENTAL INVESTIGATION

Recall that we propose an SM scheme enabling a large number of OPPs while splitting after higher layers, and with controllable PPA overheads. Hence, we evaluate our scheme thoroughly regarding security as well as layout cost.

Setup for Layout Assessment: Our techniques are implemented as custom procedures for *Cadence Innovus 16.15*. Our procedures impose negligible runtime overheads. We use the *Nangate 45nm Open Cell Library* [21]; we utilize all ten metal layers. The PPA analysis has been carried out at 0.95V and 125°C for the slow process corner with a default switching activity of 0.2. Timing results are obtained by *Innovus* as well. Our ECs lift wires to M6 unless stated otherwise.

Setup for Security Analysis: We empower an attacker with the FEOL layout and with the technology libraries. We do not assume a working chip being available—it is yet to be manufactured. We utilize the network-flow-based attack provided by Wang *et al.* [12]. Other attacks such as those in [9, 10] have not

TABLE II

TOTAL NUMBER OF OPPs WHILE SPLITTING AFTER M5. FOR A FAIR COMPARISON, HERE WE LIFT WITHOUT LOSS OF GENERALITY 30% OF THE NETS FOR ALL BENCHMARKS AND STRATEGIES.

Benchmark	OPP			
	Original	Naive Lifting	Strategies 1 and 2	Strategy 3
c432	6	67	86	103
c880	8	116	170	204
c1355	6	120	147	164
c1908	13	142	219	269
c2670	112	228	356	315
c3540	53	386	576	458
c5315	196	582	845	780
c6288	38	1,235	1,590	1,630
c7552	127	533	900	795

been available to us at the time of writing.⁷ Functional equivalence was validated using *Synopsys Formality*. The OER and HD are calculated using *Synopsys VCS* by applying 100,000 random input vectors.

Benchmarks: We conduct our comprehensive experiments using in total 28 benchmarks, selected not only from the “traditional” suites (i.e., *ISCAS-85*, *MCNC*, and *ITC-99*), but also from the large-scale *IBM superblue* suite [22]. For the latter, we leverage scripts from [23] to generate LEF/DEF files, but we also use the *Nangate 45nm* library [21] while doing so.

Setup for Comparisons: The unsplit but protected, full layouts of [12, 15] have been provided to us as DEF files. However, we were not made aware of (i) the intended split layer, (ii) the selection of protected nets, or (iii) the library files. As for (i), there are indications in the layouts that they have been tailored for splitting either after M3, M4, or M5. Hence, we calculate any comparative PNR values as average over those layers. As a result of (ii), we cannot verify the other metrics but simply quote them from the respective publications. Because of (iii) we cannot contrast PPA numbers.

Public Release: We provide our EC implementation in [14], enabling others to protect their layouts likewise. Moreover, we provide our final layouts as reference cases as well in [14].

A. Security Analysis

Increase in OPPs: Recall that more OPPs helps make proximity attacks challenging, which is corroborated by a reduction in PNR (Figs. 3 and 4). From our exploratory comparison of lifting strategies in Table II it is apparent that our strategies successfully increase the number of OPPs over both original layouts and layouts where naive wire lifting is employed.

As it depends on the benchmark whether the lifting of Hi-FONs and long nets (Strategies 1 and 2) or short nets (Strategy 3) induces more OPPs, we suggest to apply our strategies in conjunction, as proposed in Sec. IV. Next, we confirm the superior resilience of our strategies while evaluating the PNR.

On the Effectiveness of Our Scheme: Fig. 11 compares the PNR for (i) naive lifting, (ii) lifting using our Strategies 1 and 2, and (iii) lifting using our Strategy 3. For a fair and comprehensive comparison, as with the exploratory comparison of induced OPPs above, here we lift the same percentage of nets

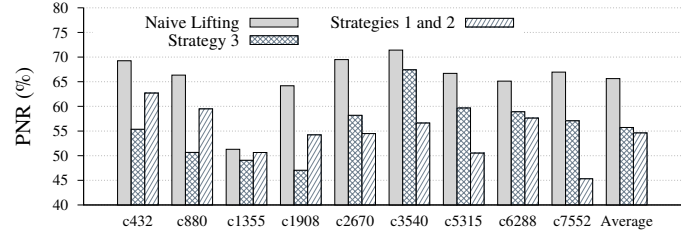


Fig. 11. Comparison of PNR values for naive lifting and our proposed strategies. The attack is based on [12]. The data reflects the average recovery/piracy rate for splitting layouts after M3, M4, and M5.

TABLE III

COMPARISON WITH [15] ON AVERAGE PNRs (OVER M3, M4, AND M5) FOR THE SAME NUMBER OF NETS SELECTED FOR PROTECTION. THE ATTACK IS BASED ON [12].

Benchmark	Protected Nets	PNR for [15]	PNR for Proposed Scheme
c432	34	87.5	70.7
c1355	74	84.8	60.1
c1908	56	91.2	58.9
c7552	66	93.9	70.2

(i.e., 30%) for all benchmarks. We derive the average PNR while splitting the layouts after M3, M4, and M5.

We achieve an improvement (i.e., reduction of PNR) of 10–11% for our strategies over naive lifting on average. Also here we observe that it depends on the benchmark which lifting technique is more effective. Thus, we apply our techniques in conjunction for all remaining experiments—this helps to lower PNR values even further (see below and Table IV).

Comparison with Prior Art: Initially, as a baseline comparison to the most recent work of Wang *et al.* [15], we protect the same number of nets as they do, but the actual selection of nets to protect/lift is based on our strategies. We achieve an average improvement of $\approx 24\%$ for the PNR here (Table III).

In Table IV, we contrast the schemes of [12, 15] and our regular scheme, where the scope for protection/wire lifting depends on the allocated PPA budgets (see also Subsec. B).

Naturally, original layouts without any protection are most vulnerable, and an attacker recovers 96% of the netlist on average. Constrained placement perturbation as proposed in [12] provides only little improvement, reducing the average PNR to 95%. That is because routing eventually compensates for any gate-level perturbation, with small displacements typically being re-routed in lower metal layers (which may be readily available to an attacker). The routing-centric scheme of [15] can lower the PNR to 88.5%. In contrast, our scheme offers significantly better protection—with 31% PNR on average, the resilience improves by 57–64% over the prior art of [12, 15].

Besides the comparison based on our PNR metric, we also contrast our scheme using established metrics (Sec. V). As for the CCR, we note that the approach of [12] provides again only little improvement (2.4%) over unprotected, original layouts. The scheme of [15], however, achieves an improvement of 21.9%, reducing the average CCR to 72.4%. Also here, our approach provides superior protection, by means of 0% CCR. Our scheme further achieves an optimal OER of 100% (as is [15], but not [12]). Finally, we observe an average HD of 40.3%. This translates to improvements of 25% and 11% over [12] and [15], respectively, despite the fact that we do not specifically target for optimal HD (50%) in our scheme.

⁷Given the focus on academic tools in [9, 10], we further assume that these attacks are not readily compatible with our industrial design flow.

TABLE IV

COMPARISON WITH ORIGINAL LAYOUTS AND PRIOR ART. WE CALCULATE ALL PNR VALUES AS AVERAGE OVER SPLITTING LAYOUTS AFTER M3, M4, AND M5. CCR, OER, AND HD VALUES FOR ORIGINAL LAYOUTS, [12], AND [15] ARE ALL QUOTED FROM [15]; CCR IS DERIVED AS $(100\% - \text{ICR})$. WE ALSO REPORT OUR PPA COST. ALL VALUES ARE IN PERCENTAGE. THE ATTACK IS BASED ON [12].

Benchmark	Original Layout				Placement Perturbation [12]				Routing Perturbation [15]				Proposed Scheme						
	PNR*	CCR*	OER	HD	PNR	CCR	OER	HD	PNR	CCR	OER	HD	PNR	CCR	OER	HD**	Die-Area Cost	Power Cost	Delay Cost
c432	97.9	92.4	75.4	23.4	95.1	90.7	98.8	41.8	87.5	78.8	99.4	46.1	32.3	0	100	45.9	7.7	13.1	11.6
c880	100	100	0	0	95.3	96.8	15.8	1.2	86.8	47.5	99.9	18.0	28.3	0	100	39.8	0	12.1	19.9
c1355	98.3	95.4	59.5	2.4	97.2	93.2	94.5	8.0	84.8	77.1	100	26.6	32.8	0	100	46.1	0	12.2	21.3
c1908	98.9	97.5	52.3	4.3	96.9	91.0	97.8	17.7	91.2	83.8	100	38.8	29.5	0	100	48.1	7.7	14.6	18.9
c2670	89.6	86.3	99.9	7.0	94.3	86.3	100	7.5	86.3	58.3	100	14.0	34.3	0	100	35.1	7.7	10.0	12.0
c3540	93.8	88.2	95.4	18.2	88.5	82.6	98.8	27.9	86.2	77.0	100	36.1	30.8	0	100	46.4	7.7	5.0	2.8
c5315	91.7	93.5	98.7	4.3	94.1	91.1	98.7	12.5	87.7	74.7	100	18.1	31.6	0	100	35.4	7.7	7.9	16.9
c6288	97.0	97.8	36.8	3.0	95.9	97.6	74.2	16.5	92.1	80.9	100	42.1	35.6	0	100	N/A**	27.3	12.3	15.7
c7552	93.8	97.8	69.5	1.6	97.1	97.9	81.7	3.1	93.9	73.9	100	20.3	26.9	0	100	25.7	16.7	9.3	15.7
Average	95.7	94.3	65.3	7.1	94.9	91.9	84.5	15.1	88.5	72.4	99.9	28.9	31.3	0	100	40.3	9.2%	10.7%	15.0%

* By definition, PNR and CCR values for original, unprotected layouts shall be equal. For consistency, however, we report average PNR values here as well.

** The attack of [12] tends to provide netlists with combinatorial loops, hindering their simulation. Those netlists have been post-processed using scripts of [23]. For the benchmark c6288, the post-processed netlist still fails simulation, due to “UNKNOWN” nets.

We also seek to compare with the work of Magaña *et al.* [9, 10]. However, having no access to their protected layouts of the *IBM superblue* benchmarks, we can only compare on a qualitative level. In Table V, we contrast their and our counts of *additional vias* above their assumed split layer, i.e., M4, and up to M6, where we lift wires to in our scheme. Note that only the total via counts across all layers before lifting and the layer-wise differences in via counts after lifting are given in [9], but not the original via counts per layer. Considering the respective total via counts before lifting as independent base-lines, our scheme increases the vias for V45 and V56 by 2.25–3.71% (with respect to total vias), whereas Magaña *et al.* increase those vias counts only by 0.67–2.03%.

In their recent study [10], Magaña *et al.* also report on the relative vias increases per layer; we contrast their increases with ours in Table VI. We observe on average 74% and 101% more vias for V45 and V56, respectively, while the respective increases reported in [10] are roughly only 16% and 49%. Note that we achieve the underlying wire lifting while keeping the die area fixed as in [10], i.e., we induce zero area cost (and only marginal power and delay overheads, see also Subsec. B).

Any increase of vias above the split layer is a direct indication of more nets being routed in the BEOL, hence inducing more OPPs and a higher complexity for proximity attacks. Therefore, we believe that our scheme generally renders the *IBM superblue* benchmarks more resilient.

B. PPA Analysis

Recall that we cannot directly compare to the works of Wang *et al.* [12, 15] (and Magaña *et al.* [9, 10]). That is because we have no access to the library (and DEF) files, and PPA cost are not reported in the respective publications. As for our qualitative comparison with Magaña *et al.* [9, 10], we also report our PPA numbers on the large-scale *IBM superblue* benchmarks (Table V). Notably, we observe only 0.85%, 0.83%, and 0% overheads for power, delay, and die area, respectively.

We next discuss in detail the PPA cost as incurred for the comparative experiments (Subsec. A, Table IV). Empirically, we allow for different PPA budgets since large benchmarks such as c6288 require more die area to maintain DRC-fixable layouts (and reasonably low PNR values). The average budgets for the experiments in Table IV are 10% for power and

die area, and 15% for delay, respectively. Using our flow and given these budgets, we can lift on average 50–60% of all nets. This ratio of lifted nets over PPA budgets is reasonable—that is especially true in contrast to naive lifting (Fig. 5).

On Area: Recall that our elevating cells do not impact the FEOL area. Besides, we initially set the utilization targets such that less than 1% routing congestion can be obtained. Whenever required to enable lifting, we stepwise increase die outlines, which is then reported as die-area cost.

On Power and Performance: As we move selected nets to higher metal layers, an increase of wirelength is expected. As a result, we also observe average overheads of 10.7% and 15.0% for power and delays, respectively. One can attribute those reasonable overheads to the relatively low resistance of higher layers. Once more and more nets are lifted, however, that positive effect is offset by a steady increase of routing congestion. Typically, congestion is managed by re-routing, which lengthens nets further, aggravating the overheads further to some degree. Besides, we conservatively estimate the impact of dummy OPPs. That is because we consider the annotated load of ECs, capturing the wires and sink, whereas only the capacitance of the dangling wire has to be driven in reality.

On the Use of Additional Metal Layers: Finally, we observe that the PPA cost (and PNR) can be further improved once additional metal layers are employed (Table VII). Here we duplicate M6 two times, resulting in 12 layers in total. Also, here we focus on relatively large and challenging benchmarks.

Additional metal layers can even provide a commercial benefit for SM and wire lifting, as long as higher layers are used. That is because the relatively low mask and manufacturing cost of large-pitch, higher layers may be more than compensated for by the achievement of zero cost for die area—this reduces the overall footprint of SM on commercial cost significantly.

VII. CONCLUSION

We propose a BEOL-centric scheme towards concerted wire lifting, advancing the prospects of split manufacturing (SM). Besides, our novel PNR metric helps to properly quantify the resilience against gate-level theft of intellectual property (IP).

The objectives we addressed here are (i) to enable splits after higher metal layers, thereby reducing the commercial footprint

TABLE V

COMPARISON WITH [9]. FOR FAIR COMPARISON, WE ALSO ALLOW NO DIE-AREA OVERHEAD. WE REPORT PPA NUMBERS ON DRC-CLEAN LAYOUTS.

Benchmarks			Implicit Wire Lifting [9]			Proposed Scheme					
Name	Nets*	Placement Util. (%)	Total Vias* Before Lifting	Δ +V45 After Lifting	Δ +V56 After Lifting	Total Vias* Before Lifting	Δ +V45 After Lifting	Δ +V56 After Lifting	Power (mW) After / Before	Delay (ns) After / Before	Die Area (μm^2) After = Before
<i>superblue1</i>	879,168	69	4,597,616	40,051 (0.87%)	70,355 (1.53%)	6,679,733	247,739 (3.71%)	233,749 (3.50%)	82.7 / 81.9	29.8 / 29.4	1,520,868
<i>superblue5</i>	764,445	77	4,650,756	34,828 (0.75%)	62,704 (1.35%)	5,523,805	139,900 (2.53%)	133,052 (2.41%)	79.2 / 78.6	24.7 / 24.6	1,298,221
<i>superblue10</i>	1,158,282	75	6,304,110	42,210 (0.67%)	50,999 (0.81%)	8,875,439	228,454 (2.57%)	220,176 (2.48%)	116.3 / 115.5	29.8 / 29.5	2,176,080
<i>superblue12</i>	1,523,108	56	8,913,075	151,018 (1.69%)	175,614 (1.97%)	11,813,683	265,992 (2.25%)	274,908 (2.33%)	127.2 / 126.3	28.9 / 28.8	2,276,426
<i>superblue18</i>	672,084	67	3,582,687	45,417 (1.27%)	72,897 (2.03%)	4,852,381	164,971 (3.40%)	163,412 (3.37%)	81.3 / 80.4	19.7 / 19.5	1,158,182

* Values are different as we use *Cadence Innovus* whereas Magaña *et al.* [9] employ academic tools. Moreover, the metal layer corresponding to M10 in the *Nangate 45nm* library [21] is missing for [9]. As the contribution for overall routing tracks from M10 is only 1.41%, the comparison can be considered fair nevertheless.

TABLE VI

COMPARISON WITH [10]. NOTE THAT OUR LAYOUTS ARE THE SAME AS FOR TABLE V.*

Benchmark	Implicit Wire Lifting [10]		Proposed Scheme		
	Δ +V45 (%)	Δ +V56 (%)	Wire Lifting (in % of Nets)	Δ +V45 (%)	Δ +V56 (%)
<i>superblue1</i>	19.18	80.10	7	101.20	133.55
<i>superblue5</i>	9.43	29.84	5	57.53	76.33
<i>superblue10</i>	26.05	54.18	5	63.97	81.93
<i>superblue12</i>	9.72	32.40	5	55.73	80.27
<i>superblue18</i>	14.32	47.41	8	91.84	135.27
Average	15.74	48.79	6	74.05	101.47

* This implies that the percentage of lifted wires is the same in Table V. We simply report it here due to lack of space in Table V.

TABLE VII

PPA COST AND PNR WHEN USING TWO ADDITIONAL METAL LAYERS. THE ATTACK IS BASED ON [12].

Benchmark	PNR	Die-Area Cost	Power Cost	Delay Cost
c5315	28.1	0	2.9	3.3
c6288	34.5	0	7.2	5.6
c7552	24.6	0	3.5	4.3
Average	29.1	0	4.5	4.4

of SM, (ii) superior resilience, and (iii) reasonable and controllable PPA cost. We believe that schemes like ours are essential to expedite the acceptance of SM in the industry.

We demonstrated exhaustively that our concerted lifting scheme is more effective and efficient than naive lifting, both in terms of protection and PPA cost. In our comparative analysis, we also found that our scheme excels prior art. For example, we achieve 0% CCR for commonly considered benchmarks (selected from *ISCAS-85*, *MCNC*, and *ITC-99* suites), whereas some prior art experiences CCR well above 70%. Besides 0% CCR, we enable PNR as low as 31% on average. This directly translates to much better IP protection than prior art, which tends to experience 89% PNR or even more. Note that we may further reduce the PNR by lifting more wires, at least once higher PPA budgets are considered as acceptable.

For future work, besides employing other upcoming proximity attacks, we will evaluate the resilience of our scheme within a formal security model. Also, we will further study the prospects of additional higher metal layers.

ACKNOWLEDGEMENTS

The authors are grateful to Yujie Wang, Tri Cao and Jeyavijayan (JV) Rajendran (Texas A&M University) for providing their network-flow attack and their protected layouts of [12, 15]. Further, the authors thank Jonathon Magaña and Azadeh Davoodi (University of Wisconsin–Madison) for discussion.

REFERENCES

- [1] C. McCants, “Trusted integrated chips (TIC),” Intelligence Advanced Research Projects Activity (IARPA), Tech. Rep., 2011. [Online]: <https://www.iarpa.gov/index.php/research-programs/tic>
- [2] B. Hill, R. Karmazin, C. T. O. Otero, J. Tse, and R. Manohar, “A split-foundry asynchronous FPGA,” in *Proc. CICC*, 2013, pp. 1–4.
- [3] K. Vaidyanathan, B. P. Das, E. Sumbul, R. Liu, and L. Pileggi, “Building trusted ICs using split fabrication,” in *Proc. HOST*, 2014, pp. 1–6.
- [4] Y. Bi, J. S. Yuan, and Y. Jin, “Beyond the interconnections: Split manufacturing in RF designs,” *Electronics*, vol. 4, no. 3, pp. 541–564, 2015.
- [5] K. Vaidyanathan, R. Liu, E. Sumbul, Q. Zhu, F. Franchetti, and L. Pileggi, “Efficient and secure intellectual property (IP) design with split fabrication,” in *Proc. HOST*, 2014, pp. 13–18.
- [6] S. Garg and J. J. Rajendran, “Split manufacturing,” in *Hardware Protection through Obfuscation*. Springer, 2017, pp. 243–262.
- [7] K. Xiao, D. Forte, and M. M. Tehranipoor, “Efficient and secure split manufacturing via obfuscated built-in self-authentication,” in *Proc. HOST*, 2015, pp. 14–19.
- [8] Q. Shi, K. Xiao, D. Forte, and M. M. Tehranipoor, “Securing split manufactured ICs with wire lifting obfuscated built-in self-authentication,” in *Proc. GLSVLSI*, 2017, pp. 339–344.
- [9] J. Magaña, D. Shi, and A. Davoodi, “Are proximity attacks a threat to the security of split manufacturing of integrated circuits?” in *Proc. ICCAD*, 2016, pp. 90:1–90:7.
- [10] J. Magaña, D. Shi, J. Melchert, and A. Davoodi, “Are proximity attacks a threat to the security of split manufacturing of integrated circuits?” *Trans. VLSI Syst.*, vol. PP, no. 99, 2017.
- [11] J. Rajendran, O. Sinanoglu, and R. Karri, “Is split manufacturing secure?” in *Proc. DATE*, 2013, pp. 1259–1264.
- [12] Y. Wang, P. Chen, J. Hu, and J. J. Rajendran, “The cat and mouse in split manufacturing,” in *Proc. DAC*, 2016, pp. 165:1–165:6.
- [13] A. Sengupta, S. Patnaik, J. Knechtel, M. Ashraf, S. Garg, and O. Sinanoglu, “Rethinking split manufacturing: An information-theoretic approach with secure layout techniques,” in *Proc. ICCAD*, 2017, pp. 329–336.
- [14] (2017) DfX Lab, NYUAD. [Online]: <http://sites.nyuad.nyu.edu/dfx/research-topics/design-for-trust-split-manufacturing/>
- [15] Y. Wang, P. Chen, J. Hu, and J. Rajendran, “Routing perturbation for enhanced security in split manufacturing,” in *Proc. ASPDAC*, 2017.
- [16] F. Imeson, A. Emtenan, S. Garg, and M. Tripunitara, “Securing computer hardware using 3D integrated circuit (IC) technology and split manufacturing for obfuscation,” in *Proc. USENIX Sec. Symp.*, 2013, pp. 495–510.
- [17] M. Li, B. Yu, Y. Lin, X. Xu, W. Li, and D. Z. Pan, “A practical split manufacturing framework for trojan prevention via simultaneous wire lifting and cell insertion,” in *Proc. ASPDAC*, 2018, pp. 265–270.
- [18] Z. Chen, P. Zhou, T.-Y. Ho, and Y. Jin, “How secure is split manufacturing in preventing hardware trojan?” in *Proc. AHOST*, 2016, pp. 1–6.
- [19] S. Patnaik, M. Ashraf, J. Knechtel, and O. Sinanoglu, “Obfuscating the interconnects: Low-cost and resilient full-chip layout camouflaging,” in *Proc. ICCAD*, 2017, pp. 41–48.
- [20] A. B. Kahng, J. Lienig, I. L. Markov, and J. Hu, *VLSI Physical Design: From Graph Partitioning to Timing Closure*. Springer, 2011.
- [21] (2011) NanGate FreePDK45 Open Cell Library. Nangate Inc. [Online]: http://www.nangate.com/?page_id=2325
- [22] N. Viswanathan, C. J. Alpert, C. Sze, Z. Li, G.-J. Nam, and J. A. Roy, “The ISPD-2011 routability-driven placement contest and benchmark suite,” in *Proc. ISPD*, 2011, pp. 141–146.
- [23] A. B. Kahng, H. Lee, and J. Li, “Horizontal benchmark extension for improved assessment of physical CAD research,” in *Proc. GLSVLSI*, 2014, pp. 27–32. [Online]: <http://vlsicad.ucsd.edu/A2A/>